

## Introduction

Thermal injection Butler (1991) is an enhanced oil recovery (EOR) technique that allows significantly more oil to be extracted from a reservoir. Depletion of easily extracted oil reserves and technological advances has caused this to become a popular EOR technique.

Crude oil is heated underground by various methods such as steam injection to affect viscosity and mobility ratio resulting in yield increases up to 60%. Another EOR method, not considered in this paper, is through gas injection. With thermal methods steam is injected into oil wells to improve oil production rates and enhance oil recovery by decreasing oil viscosity. The implementation of oil recovery by steam injection requires a good knowledge of the subsurface thermal conditions. Temperature observation wells (TOW) are used to measure subsurface temperature profiles which can be used to define the vertical thickness of the steam flood, area sweep, rate of heat flow and heat losses to surrounding rock layers. When trying to enhance oil recovery from heavy oilfields, operators may take temperature measurements once every 90 to 180 days for each TOW location. The cost of conducting this invasive down hole thermometer measurement is around \$5,000 per well, in addition to the upfront drilling cost. During measurement the wells are not in production and there is additional cost associated with this downtime. Problems arising between TOW temperature measurements can go undetected and cause significant problems.

In this article we present a noninvasive method for the remote monitoring of subsurface temperature using low frequency radar pulses. Conventional ground penetrating radar Jol (2009) has limited applications for subsurface measurements in oil fields due to electromagnetic losses, which are rather high in the commonly used frequency range of 50 – 1000MHz, resulting in a rather shallow exploration depth. Deeper penetration up to several kilometers has been achieved with much lower frequencies (1 – 5Mhz) using very large antenna's in resistive environments such as Martian rock, ice, and permafrost Bertheliet et al. (2005); Angelopoulos et al. (2013). We present results using the Adrok radar system Stove and van den Doel (2015) which emits a multispectral wave packet with significant energy in the low 1 – 5Mhz band van den Doel et al. (2014) for increased penetration depth which is in our experience sufficient to reach the comparatively shallow hot zones where steam was injected.

The ADR signal generator produces a pulse of electromagnetic energy (frequencies typically range between 1MHz to 70MHz) that is fed to the antenna and is transmitted into the ground. Once the signal has been sent to the transmitting antenna a signal is sent to the receiving control unit to synchronise collection of the subsurface reflected data, which is collected through the receiving antenna and then digitized. The transmitted pulse is depicted in Figure 1 where we also show the power spectrum. It is not the usual localized pulse with a single centre frequency but a more complicated waveform. The higher frequency components allow accurate localization at shallow depths, but attenuate rapidly in the ground, while the lowest frequency component around 3Mhz can penetrate much deeper. We thus combine the advantage of high spatial resolution at high frequencies with the advantage of greater depth penetration at low frequencies at the expense of requiring more sophisticated analysis.

Radar surveys were performed at 64 locations near TOWs in 3 oilfields and returns were correlated, after signal processing Stove et al. (2018) described below, with measured down hole temperatures by training a feedforward neural network. The results were evaluated by excluding one of the data pairs from training and use a network trained on the remaining wells to predict the excluded site, resulting in blind tests. We believe results are encouraging, though not yet fully reliable and we discuss avenues for improvements.

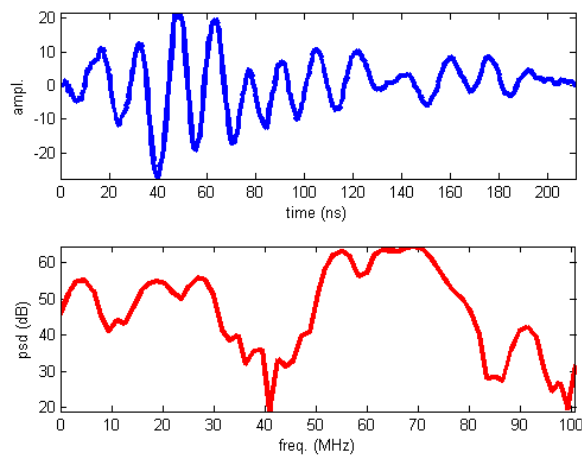


**Figure 1** Transmitted pulse and its power spectral density.

## Measurements

Radar scans were performed near TOWs at three operational oilfields, referred to here as sites A, B, and C. At site A we obtained 21 measurements, at site B 40 and at site C 3. Each site has approximately homogeneous subsurface geology, but the sites themselves differ.

Each scan consisted of the emission of a low frequency pulse and detection of returns as time domain traces recorded digitally. At each location over 100,000 traces were taken for noise reduction through stacking. A velocity model based on a calibration site was used for time to depth conversion up to 1900ft which is the largest depth for which TOW data was available.

Changes in subsurface temperature will affect conductivity and permittivity Kummerow and Raab (2015), which will affect the radar returns. Due to the diffuse nature of the temperature gradients we will not see sharp reflections as in conventional subsurface imaging with GPR or seismic but more complicated effects. Initial analysis of the data set suggested the *modulation* Mather and Koch (2011) widely used in remote sensing, as a candidate parameter to correlate with temperature. Variations in subsurface geology will also affect results and we disentangle these effects from temperature effects through machine learning.

## Analysis

Modulation (M) and TOW temperature data (T) were down sampled to a 50ft grid and the available (M,T) pairs, except the target, were used to train a feedforward neural network to predict the target T. Once trained the neural network should extract the temperature from the radar data which contains a mix of features caused by the temperature gradients and by the geology. As the geology differs significantly between the three sites, separate networks were trained for sites A and B, referred to as the A-net and B-net. Training the network for site C is not useful as we have only 3 data pairs.

In Figure 2 and 3 we display the measured modulation ( $0 \leq M \leq 1$ ) derived from the radar scans and the measured TOW temperature for site A and site B, where migration from time to depth was performed using a velocity model from a calibration site.

Due to the small training set a principled approach Goodfellow et al. (2016) using training, validation, and testing sets is not feasible and we proceeded more heuristically, experimenting

with various stopping criteria for training and network architectures. Best performance was found using a 5 layer network with 3 hidden layers with 15 units, stopping training (using standard backpropagation gradient descent) at 500 iterations. Minor changes to this architecture do not affect the results very much. Small changes in results can be observed depending on the (random) initialization of the network weights, as the optimization (training) is highly non convex. To reduce this variability we have averaged results over 100 independently randomized network initializations.

The results for site A and C are depicted in Figure 4, The plots 1 – 21 represent blind tests for those specific wells, using a network trained on the other 20 wells. The last three plots, shaded green, show the result obtained by applying net-A trained on all 21 sites to predict the temperature profiles for the 3 wells of site C. For comparison we also show the results using a smaller network with only one hidden layer in Figure 5, which is comparable though a little worse.

The results for site B are depicted in Figure 6. Each plot is a blind prediction using a network trained on the other 39 sites only.

## Discussion

Examining the results for site A and C in Figure 4 we note that the results from site C (shaded green) are negative, whereas the site A results are mostly qualitatively correct. This demonstrates that the modulation  $M$  is determined by the geology as well as the temperature, because geology is the main difference between the sites. Focusing on site A only, 1 – 3 are quite good, correctly identifying the steam injection location around 1300ft and the temperature curve is matched quite well, though the actual temperature is underestimated. 4 – 6 correctly identify the hot zone at the correct depth, but the steep gradient around 600ft was missed. The cold locations 7 – 9 correctly show a more or less constant low temperature, with 8 deviating most in the shallow region. Temperature profiles in 10 – 12 show a lukewarm zone around 1000ft, which shows up in 10 but not in the others. 13 – 15 follow the ground truth quite well, but ramping up a bit too slow. The hot zone in 16 – 18 appears about 100ft too deep, and maximum temperature is underestimated. TOW data for 19 – 21 is missing most of the hot zone apparently around 1500ft (deeper TOW data was not available), and the hot zone is identified around 1300ft in 19 and 21, and missed altogether in 20.

Turning to site B in Figure 6 we note that at some wells such as 2 and 20 we have a very good fit, at some wells like 11 and 13 the predicted hot zone has a significant depth error, and at some wells like 24 and 38 the prediction fails altogether.

The large variability in the quality of the reconstructions can be explained by local variations in geology or other subsurface anomalies. If additional data pertaining to the subsurface structure of each well were made available to the network this problem could perhaps be solved resulting in more reliable predictions.

Another approach circumventing this problem would be to use independent machine learning for each individual well for time-lapse monitoring. This would restrict use of this method near wells with a TOW, where after an initial temperature log taken in the usual way, a network is trained to correlate radar returns for that specific site, then obtain radar measurements, which is significantly cheaper than acquiring a temperature log and is non-invasive, at shorter intervals than 90 – 180 days. If changes are observed in the predicted temperature profile for a specific well this could indicate a problem and another temperature log from the TOW could be taken, potentially detecting the problem months before it would show up using the normal temperature

measurement schedule.

## Conclusions

Results presented here indicate that the modulation derived from the radar traces contains information about the subsurface temperature, and could potentially be used to remotely measure temperature accurately if all other subsurface features were the same. Variation in the quality of results, in particular comparing site C reconstructions with site A reconstructions suggest the method could be improved by incorporating more information in the machine learning, in particular subsurface geology.

Another obvious source of inaccuracy is the small size of the training set which can be increased by taking more measurements. A complementary approach is to use physical simulation of the process to create simulated training data, allowing large training sets to be constructed. This approach requires accurate physical models and as electromagnetic properties of earth materials are notoriously complex, and difficult to measure in situ, this will pose challenges for further research.

It would be interesting to apply this methodology to other EM subsurface measurement methods such as resistivity surveys which should also be able to see a relation between resistivity and temperature which perhaps could be disentangled from the geological features.

## References

- Angelopoulos, M.C., Pollard, W.H. and Couture, N.J. [2013] The application of CCR and GPR to characterize ground ice conditions at Parsons Lake, Northwest Territories. *Cold Regions Science and Technology*, **85**, 22–33.
- Berthelier, J.J., Bonaime, S., Ciarletti, V., Clairquin, R., Dolon, F., Gall, A.L., Nevejans, D., Ney, R. and Reineix, A. [2005] Initial results of the Netlander imaging ground-penetrating radar operated on the Antarctic Ice Shelf. *GEOPHYSICAL RESEARCH LETTERS*, **32**(L22305), L22305, doi:10.1029/2005GL024203.
- Butler, R. [1991] *Thermal Recovery of Oil and Bitumen*. Englewood Cliffs, N.J.: Prentice Hall.
- van den Doel, K., Jansen, J., Robinson, M., Stove, G.C. and Stove, G.D.C. [2014] Ground penetrating abilities of broadband pulsed radar in the 1-70MHz range. In: *SEG Technical Program Expanded Abstracts 2014, Denver*. 1770–1774.
- Goodfellow, I., Bengio, Y. and Courville, A. [2016] *Deep Learning*. MIT Press.
- Jol, H.M. [2009] *Ground Penetrating Radar Theory and Applications*. Elsevier, Amsterdam.
- Kummerow, J. and Raab, S. [2015] Temperature Dependence of Electrical Resistivity Part II: A New Experimental Set-up to Study Fluid-saturated Rocks. *Energy Procedia*, **76**, 247–255.
- Mather, P.M. and Koch, M. [2011] *Computer Processing of Remotely-Sensed Images*. John Wiley and Sons, Ltd., London.
- Stove, G. and van den Doel, K. [2015] Large depth exploration using pulsed radar. In: *ASEG-PESA Technical Program Expanded Abstracts 2015, Perth*. 1–4.

Stove, G., Stove, G.C. and Robinson, M. [2018] New method for monitoring steam injection for Enhanced Oil Recovery (EOR) and for finding sources of geothermal heat. In: *Australian Exploration Geoscience Conference*.

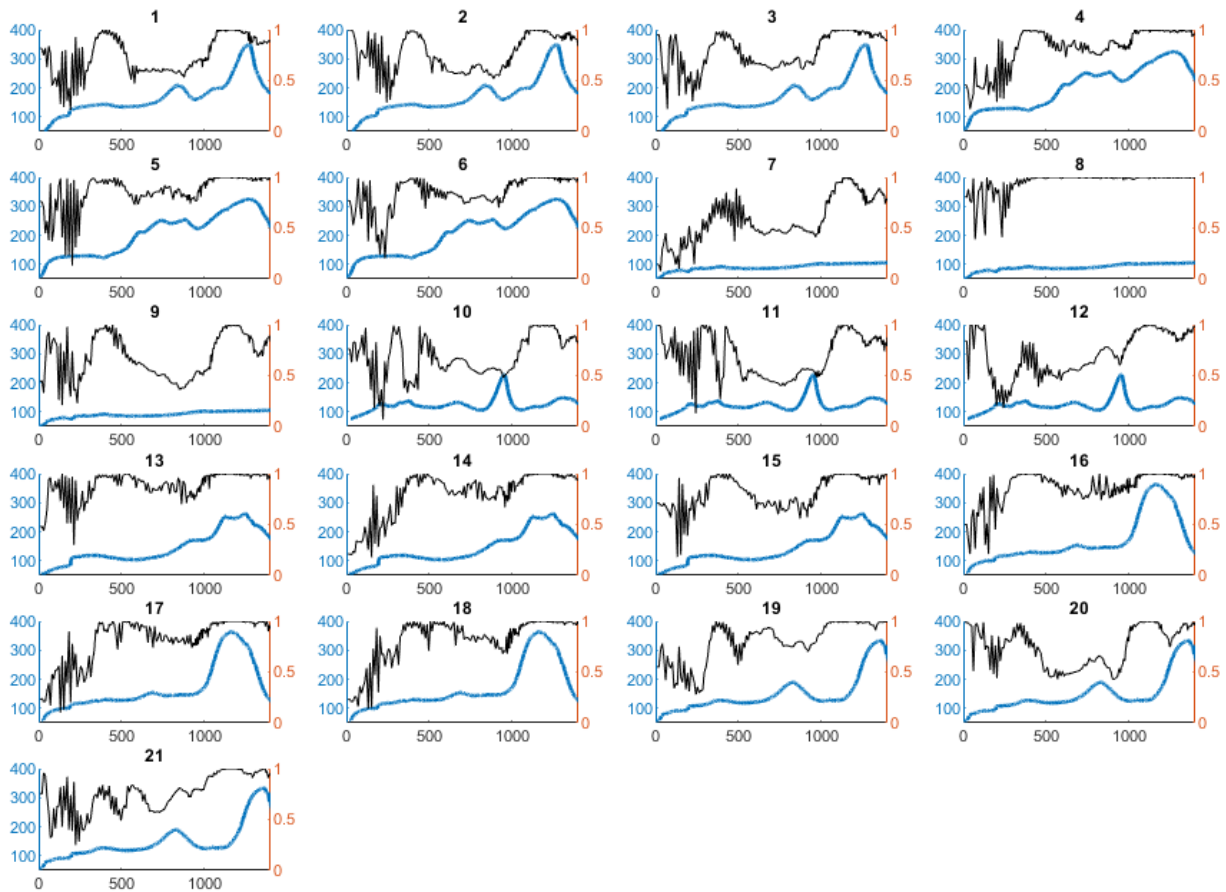


**Figure 2** Modulation (black) and temperature in Fahrenheit (blue) versus depth in feet for 21 training holes at site A.

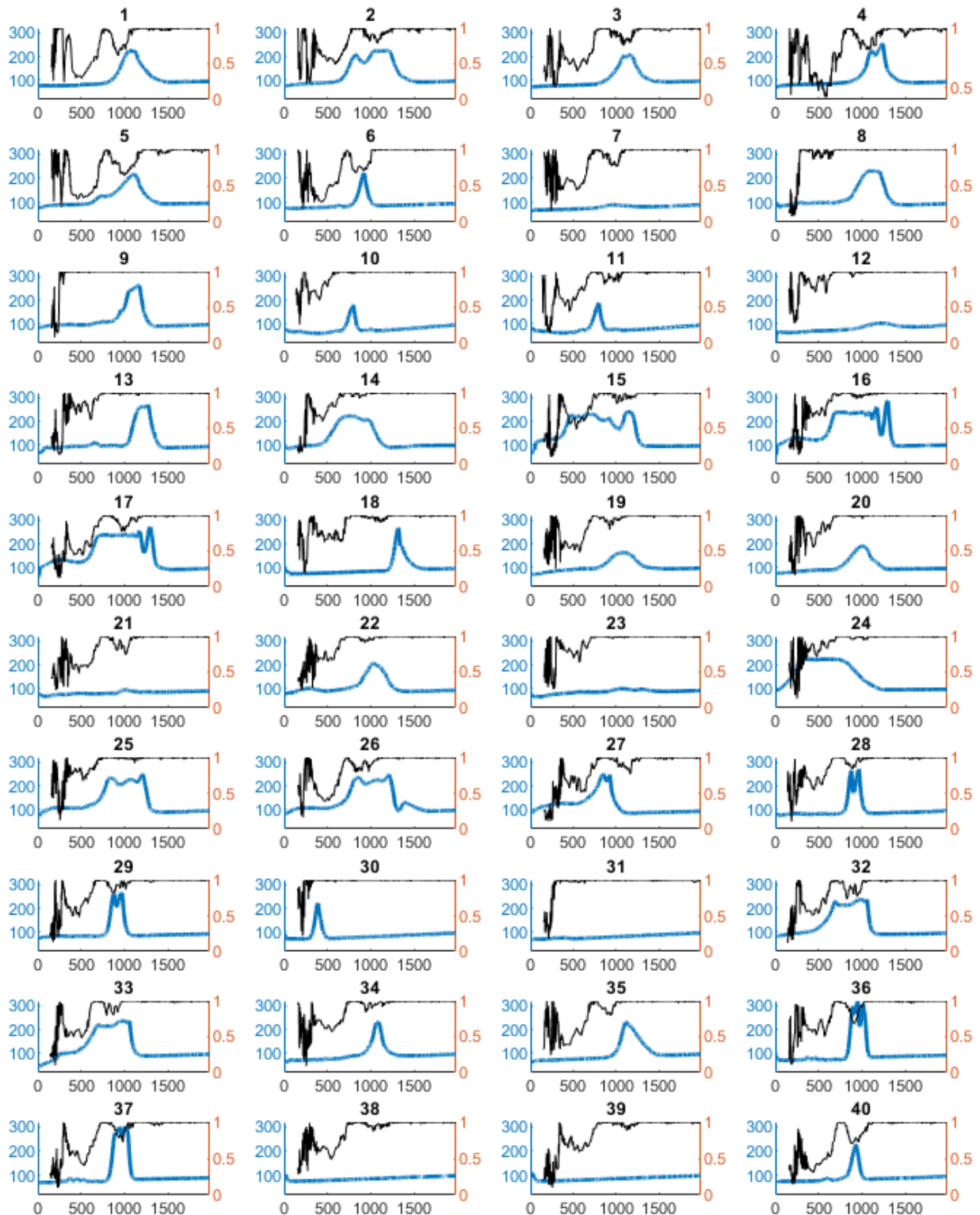


**Figure 3** Modulation (black) and temperature in Fahrenheit (blue) versus depth in feet for 40 training holes at site B.

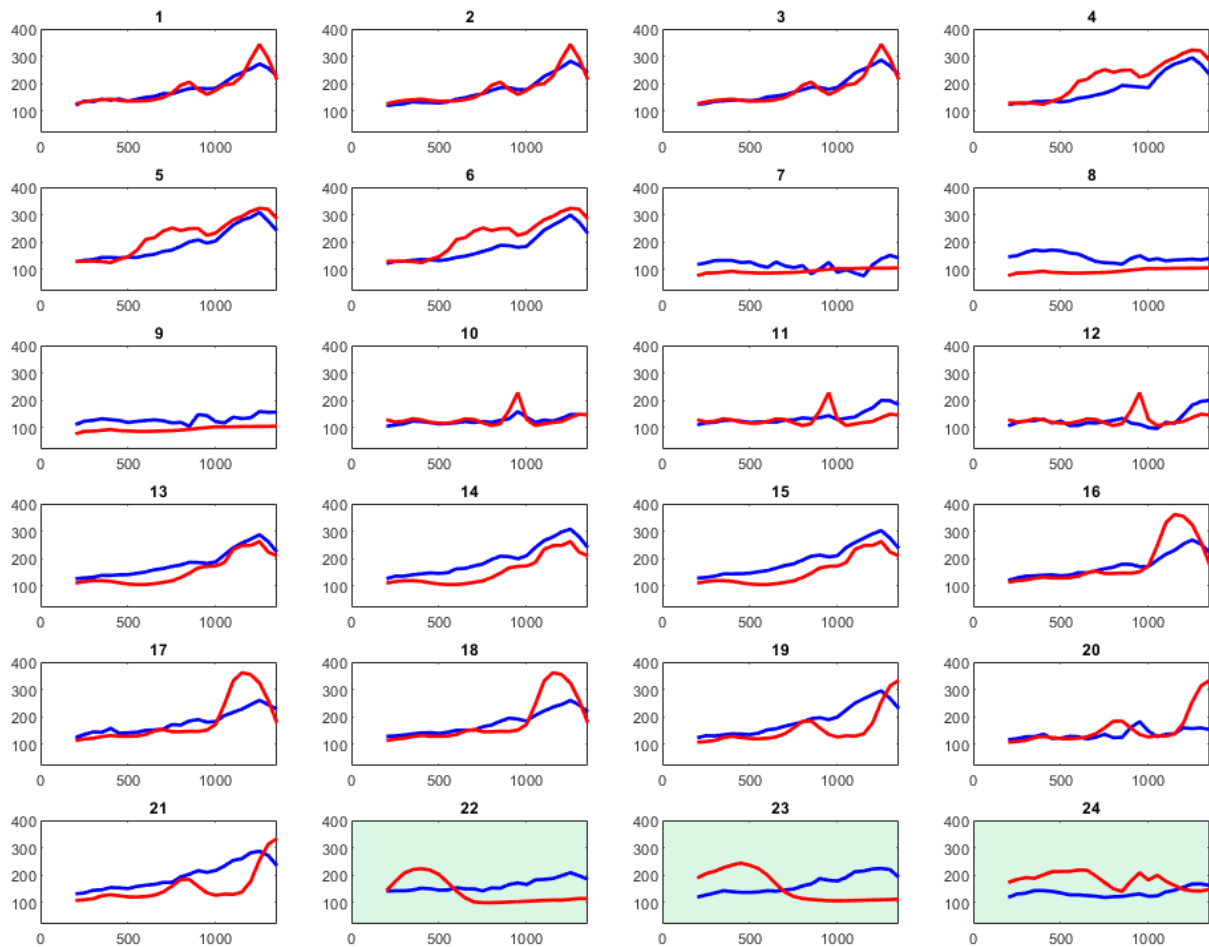


**Figure 4** Reconstructed temperature (blue) and TOW measured temperature (Fahrenheit) versus depth (feet) for site A and C. Each location from site A (1 – 21) was trained using 20 modulation-temperature pairs, excluding the location itself. The last 3 plots used all site A data sets for training and used this to predict temperatures for 3 locations at site C, which has different geology.

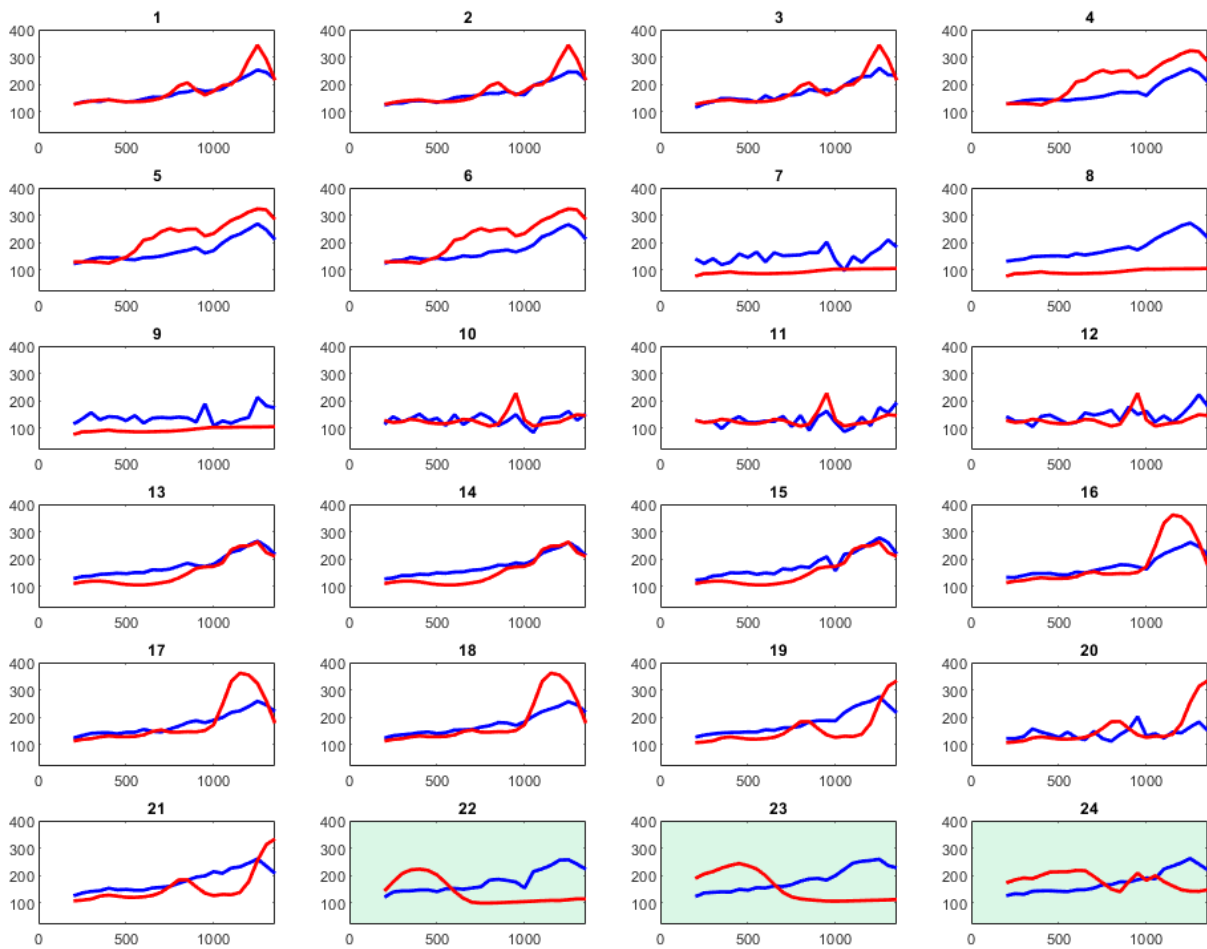


*Figure 5 Same results as Figure 4 using a smaller neural network with only one hidden layer.*

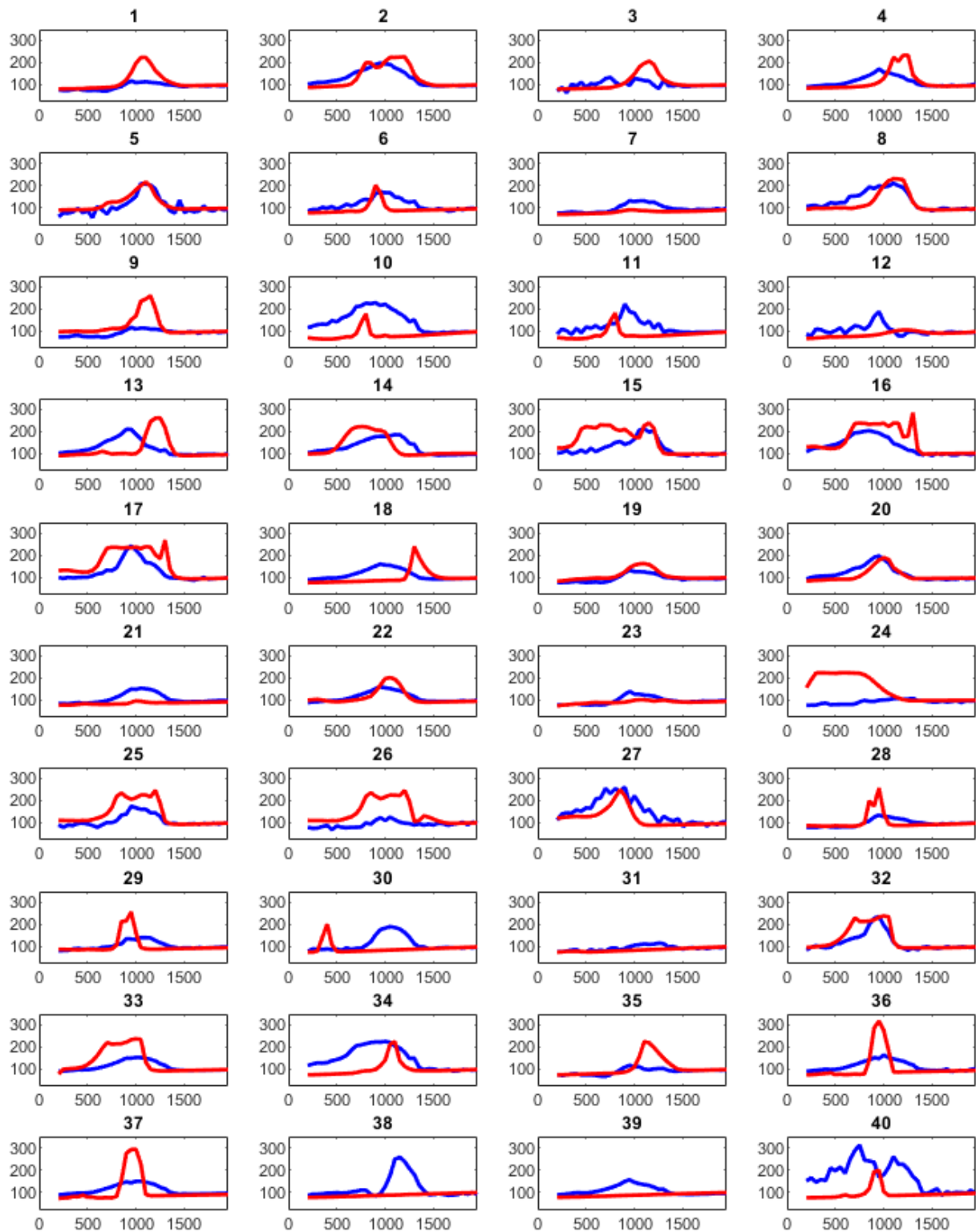


**Figure 6** Reconstructed temperature (blue) and TOW measured temperature (Fahrenheit) versus depth (feet). Each location from site B was trained using 39 modulation-temperature pairs, excluding the location itself.